

Hurricane influence on the oceanic eddies in the Gulf Stream region

Received: 23 August 2024

Xinning Ni ^{1,2}, Yu Zhang ^{1,2}  & Wei Wang ^{1,2} 

Accepted: 6 January 2025

Published online: 10 January 2025

 Check for updates

The Gulf Stream region (GSR) represents an area of robust oceanic eddies, active hurricanes, and more importantly, frequent encounters between the two phenomena. However, the direct impact of the intense storms on the eddy field has seldom been comprehensively examined. Here based on a multi-year analysis of eddy energy changing rate, we demonstrate that hurricanes enhance cyclonic eddies but weaken anticyclonic ones by injecting potential vorticity into the ocean. Such effects are not only pronounced immediately following hurricane-eddy encounters, but also retained for extended periods within large eddies that have long lifespans. Consequently, the variation of the annual mean energy and vorticity of the eddy field exhibits a high correlation with hurricane intensity. It can thus be argued that hurricanes over the GSR play an important role in driving the long-term variation of the underlying eddy field, thereby affecting ocean circulation and climate.

The Gulf Stream (GS) and its extension are pivotal in modulating the Earth's climate patterns and sustaining the ecological systems^{1–4}. They act as both a western boundary current (WBC) system for the wind-driven North Atlantic subtropical gyre⁵ and a key component of the Atlantic meridional overturning circulation (AMOC)⁶. The Gulf Stream region (GSR), defined here as the domain spanning 40°–80°W and 25°–45°N, is distinguished by one of the most energetic eddy fields in the world oceans (Fig. 1a). The term eddies here is used to describe not only strong meanders of the main current but nonlinear, isolated structures that rotate at a faster rate than they move, thereby enabling them to transport water and other properties over long distances^{7,8}. Examples of such structures include the large, deep-reaching warm-core rings and cold-core rings that are best known for the GS system^{9,10}. Recent studies have suggested that the interaction between oceanic eddies and the atmosphere at mesoscales in WBCs is essential to the dynamics and variability of both ocean and atmosphere circulation^{11–13}. In particular, the interaction between eddies and hurricanes has been revealed to exert a large impact on the Kuroshio transport¹⁴. Whether a similar process plays a role in the GSR is of great interest, but remains unclear.

In the North Atlantic, strong hurricanes are not rarely seen in the mid-latitude¹⁵. Probably due to the generally warmer sea surface

temperatures (SSTs) compared with other ocean basins, hurricanes in this region attain their lifetime maximum intensity as far north as 30°N (ref. 16). Regarding the overall hurricane activity, as measured by power dissipation index (PDI)¹⁷, the high-value area extends northwards from low latitudes till across the edge of GSR (Fig. 1b). During hurricane seasons, oceanic eddies routinely encounter intense hurricanes, and eddy-hurricane interactions ensue¹⁸. While considerable evidence from models and observations indicates that preexisting oceanic eddies affect hurricane evolution by regulating the upper ocean thermal response^{18–21}, the general response of the eddy field to hurricanes remains largely uninvestigated.

The impact of hurricanes on oceanic mesoscale eddies can occur through two distinct pathways: direct and indirect. The direct influence of hurricanes on eddies acts through two primary mechanisms¹⁴. Firstly, hurricane-induced strong surface currents have the potential to perturb the eddies out of geostrophic balance, subsequently resulting in the radiation of energy from the eddies in the form of gravity waves at the inertial frequency²². The eddies thus exhibited an accelerated decay rate above the background mean level. In addition to the aforementioned process, which results in a similar response in cyclonic and anticyclonic eddies, another mechanism can generate contrasting outcomes in these two types of eddies. Through the action of

¹Key Laboratory of Physical Oceanography and Frontiers Science Center for Deep Ocean Multispheres and Earth System/Academy of Future Ocean, Ocean University of China, Qingdao, China. ²Qingdao National Laboratory for Marine Science and Technology, Qingdao, China. ✉ e-mail: yuz@ouc.edu.cn; wei@ouc.edu.cn

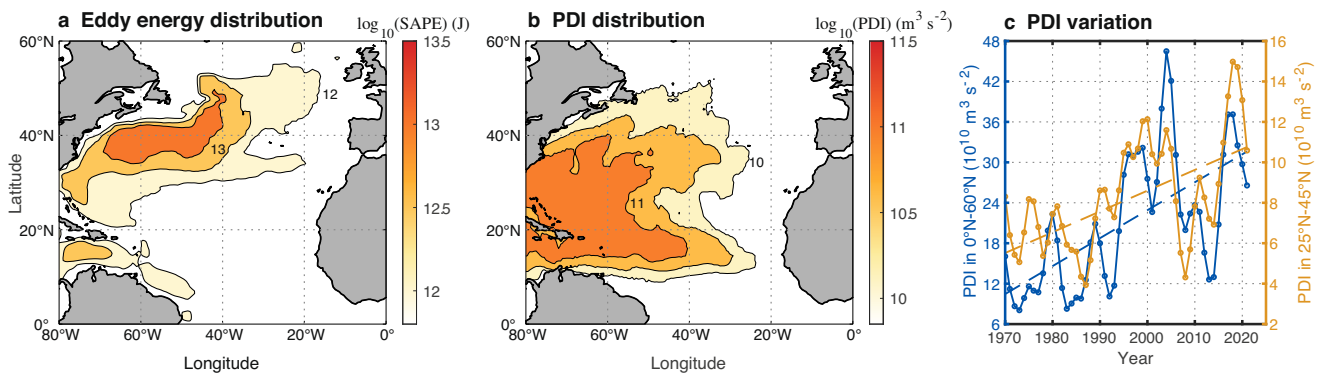


Fig. 1 | Climatological distribution of oceanic eddy energy and hurricane power dissipation index (PDI). **a** Distribution of the mean eddy's surface available potential energy (SAPE) (J) in a logarithmic scale in the North Atlantic for 1993–2021. **b** Distribution of the total hurricane PDI ($\text{m}^3 \text{s}^{-2}$) in a logarithmic scale in

the North Atlantic for 1970–2021. **c** Hurricane PDI ($10^{10} \text{m}^3 \text{s}^{-2}$) in the entire basin (blue) and in the mid-latitudes (orange) of the North Atlantic, with a 3-year running mean smoothing applied. Dashed lines denote the linear trends in a 95% confidence interval. Source data are provided as a Source Data file.

mesoscale cyclonic circulating winds or the Ekman pumping effect, hurricanes contribute positive vorticity in the form of mesoscale eddies to an eddying ocean (see Methods). This reinforces the cyclonic eddies and simultaneously weakens the anticyclonic ones^{14,23,24}. Furthermore, the process of intense hurricane-induced mixing near the ocean surface results in the formation of a prominent cold wake behind hurricanes^{25,26}. This phenomenon operates in a similar manner to the hurricane-vorticity mechanism, facilitating the formation of new cyclonic eddies, the intensification of existing cyclonic eddies, or the weakening of existing anticyclonic eddies.

Indirectly, it is evident that hurricanes have the capacity to induce remarkable disruptions and long-lasting as well as far-reaching perturbations of the GS^{27–30}. Given that GS serves as the primary energy source of mesoscale eddies through barotropic/baroclinic instability processes^{31,32}, these hurricane-induced perturbations can naturally exert an impact on the formation and evolution of the eddy field. This hurricane-GS-eddy pathway is non-local and indirect, which allows for the long-term and widespread retention of hurricane climate signals in the ocean.

As a response to the elevated level of atmospheric CO_2 in recent decades^{17,33,34}, both hurricanes in the mid-latitude North Atlantic and further south have demonstrated increasing trends ($p < 0.05$) (Fig. 1c). Furthermore, recent research indicates that intense hurricanes are migrating towards the polar regions¹⁶. These changes are likely to enhance hurricanes' role in modulating eddies over the GSR, which may, in return, affect the dynamics of the GS system and the AMOC. Prior to investigating this, it is first necessary to determine how the variations associated with hurricane activity induce changes in the underlying eddy field.

In this study, we employed North Atlantic hurricane records from the International Best Track Archive for Climate Stewardship (IBTrACS, v4r00)^{35,36}, which date back to 1850. To investigate eddy responses to hurricanes, we utilized a recently published global Mesoscale Eddy Trajectory Atlas (META3.2 DT two-sat)³⁷, derived from satellite-obtained altimetry maps for the past 30 years (1993–2021). The atlas documents the trajectories and properties of eddies that were identified based on a set of pre-established criteria, including shapes and amplitudes. Besides, the fifth generation of the European Centre for Medium-Range Weather Forecasts (ECMWF) reanalysis (ERA5)³⁸ and NCEP/NCAR reanalysis³⁹ datasets were used to assess the impact of wind and surface buoyancy flux. The RAPID-Meridional Overturning Circulation and Heatflux Array-Western Boundary Time Series (RAPID-MOCHA-WBTS)⁴⁰ at 26.5°N , from 2004 to present, was used to examine possible roles of the AMOC and the GS. The North Atlantic Oscillation (NAO) index⁴¹ was also employed to assess the

potential relation between the large-scale atmospheric variability to the eddy field.

By revealing the uniqueness of the eddy response to the vorticity forcing of hurricanes, we find that hurricanes' effects on the eddy field of GSR are strong not only during hurricane seasons, but last for an extended period afterward. The variation of the annual mean eddy field over the past 30 years exhibits a high correlation with the hurricane PDI, thereby indicating that the latter plays an important role.

Results

Eddy's short response to hurricane forcing

The aforementioned direct effects of hurricanes on eddies have been verified by observational and modeling studies^{42–44}, but mostly carried out in the western North Pacific^{14,23,24}. In the North Atlantic basin, we first identified two examples of eddy response from the sea level anomaly (SLA) field to Hurricane Hortense in September 1996 (Supplementary Fig. 1) and Hurricane Irma in September 2017 (Supplementary Fig. 2), which exhibit the strengthening of cyclonic eddies and weakening of anticyclonic eddies under the hurricane forcing. Furthermore, we performed a statistical analysis of the eddy properties immediately following their interaction with hurricanes over the past 30 years. Figure 2 depicts the mean eddy energy changing rate, averaged over a 15-day period following the hurricane-eddy encounter, in the coordinate centered on hurricanes (see Methods). Eddy responses were examined across three categories of hurricanes: tropical depression-tropical storm (TD-TS), categories 1–2 on the Saffir-Simpson scale (abbreviated as Cat 1–2), and categories 3–5 (abbreviated as Cat 3–5). In general, the responses of cyclonic and anticyclonic eddies exhibit significant differences, though both reach their peak intensity near the hurricane's center and gradually weaken outwards (Fig. 2). At approximately $r = 500 \text{ km}$, hurricanes' effects gradually diminish. This finding is consistent with the distance of hurricanes from the GS when they had an impact²⁸, and is likely related to the extent of hurricane winds.

Specifically, cyclonic eddies near the storm's center display contrasting behaviors at varying wind speeds, which are dependent on the comparative strengths of the wave-radiation-induced decaying effect and the hurricane-vorticity/mixing-induced strengthening effect. Under the forcing of TD-TS wind, cyclonic eddies undergo marked decay. As the wind gets stronger, the vorticity injection by hurricanes becomes more pronounced, thereby causing cyclonic eddies to intensify with a positive energy-changing rate, particularly in the core area (green, orange line of Fig. 2a). For hurricanes of Cat 3–5, the eddy energy growth rate can be up to three to four times greater than that under Cat 1–2 hurricanes.

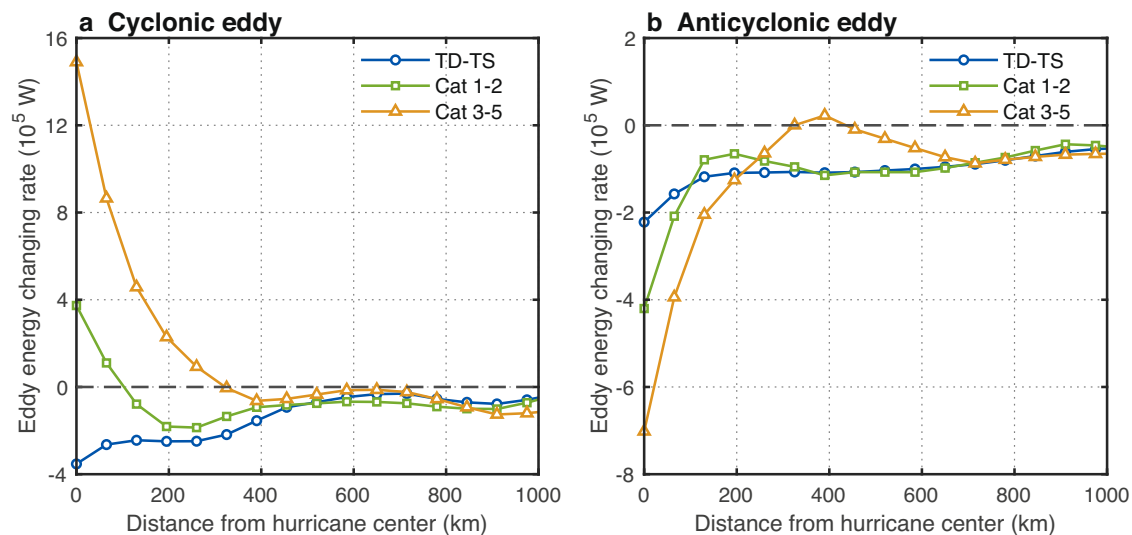


Fig. 2 | Radial distribution of eddy energy changing rate within 15 days after hurricanes' passage. a Mean energy changing rate of cyclonic eddy (10^5 W), **b** mean energy changing rate of anticyclonic eddy (10^5 W) in the North Atlantic Ocean from 1993 to 2021. Blue circle: tropical depression-tropical storm (TD-TS),

green square: categories 1–2 hurricanes (Cat 1–2), and orange triangle: categories 3–5 hurricanes (Cat 3–5). The black dashed lines denote the 0 value. Source data are provided as a Source Data file.

For anticyclonic eddies, the combined effect of the two mechanisms results in a considerable reduction in eddy energy. The magnitude of the energy-changing rate first declines sharply with distance from storm centers, and then gradually approaches the background dissipation level further away at $r \sim 1000$ km (Fig. 2b). Similar to cyclonic eddies, the energy-changing rate in anticyclonic eddies is significantly amplified under high wind speeds. Additionally, the hurricane's wind stress curl changes from positive to negative at the storm's outer edge, thereby acting to enhance anticyclones. In conjunction with the weakening effect of the wave-radiation-induced decay mechanism, the decay rate is effectively zero near $r = 400$ km (orange line of Fig. 2b).

Our findings demonstrate the two opposing effects of hurricanes on eddies in the North Atlantic Ocean. Under intense hurricanes, the hurricane-vorticity mechanism exerts a predominant influence on eddy-hurricane interactions, with a magnitude significantly greater than that under low wind speeds. Also, it manifests as opposite changes in the energy of cyclonic and anticyclonic eddies, resulting in the strengthening of cyclonic eddies and the weakening of anticyclonic ones. Furthermore, although the GS exhibits disparate dynamical features before and after its separation from the coast, which occurs around 30° N, the eddy responses to hurricanes in the two subregions demonstrate a high degree of consistency with those in Fig. 2 (Supplementary Figs. 3, 4).

Aside from hurricanes, a number of factors may affect eddies, even during the hurricane season. To have a general idea of hurricanes' significance, we then focused on year-by-year response of the eddy field in a 15-day period following the passage of hurricanes, and compared it with hurricane intensity (see Methods).

Figure 3a illustrates a strong correlation between the mean energy changing rate difference between cyclonic and anticyclonic eddies, and the PDI, with a correlation coefficient of 0.71 in a 95% confidence interval over the past 30 years. This is consistent with the multi-year mean result of the previous section, highlighting the distinctive influence of intense hurricanes in strengthening cyclonic eddies while weakening anticyclonic eddies (Fig. 2). More importantly, the mean eddy energy difference shows a close correlation with the hurricane PDI ($R > 0.8$, $p < 0.05$), undergoing substantial changes of a comparable magnitude to that of the hurricane PDI (Fig. 3b). This suggests that, among the various forces at play, hurricane forcing significantly

impacts the eddy field during hurricane seasons, resulting in substantial alterations.

It is noteworthy that our analyses of the short-term responses (15 days) of the eddies, as illustrated in Figs. 2, 3, were conducted exclusively on preexisting eddies that were already present prior to the passage of hurricanes. Therefore, the results do not include eddies that were created by the GS after hurricane disturbances. Consequently, it is not possible to discern the impact of the indirect hurricane-GS-eddy mechanism from these short-term responses. Nevertheless, the impact of the hurricane-mixing mechanism has been incorporated.

Hurricanes' impact on the long-term variation of eddy fields

Whether the imprint of hurricanes on the underlying eddy field can last long in the ocean depends on many factors, including the characteristics of the eddies themselves. Globally, the lifetime of mid-latitude eddies between 20° and 40° latitude is a function of both their horizontal scale and amplitude. Eddies with smaller amplitudes or smaller horizontal scales have shorter lifespans, whereas those with larger amplitudes or greater horizontal scales typically persist for longer periods of time. Moreover, eddies in the GSR and the Kuroshio Extension are the most energetic in the ocean, contributing to the generally longer lifespan of eddies in these two regions⁴⁵.

The energy of the eddy field in the GSR is predominantly governed by large eddies, which can live for up to 120 days or longer. In contrast, eddies with smaller horizontal scales and lower energies tend to dissipate quickly, losing the signature of hurricane forcing (Supplementary Fig. 5). Therefore, the impact of hurricanes is likely to persist over time by large eddies, leaving a long-lasting imprint in the ocean.

In light of this hypothesis, an examination was conducted of the annual mean energy of large eddies in the GSR. In recent decades, the energy of large cyclonic eddies has exhibited a multi-decadal V-shaped variation, characterized by a substantial decline until approximately 2010, followed by a large increase thereafter. Meanwhile, the energy of the large anticyclonic eddies has displayed an inverse A-shaped structure (Fig. 4a). These two contrasting multi-decadal changes are indicative of the effects of hurricanes. In particular, the hurricane PDI has

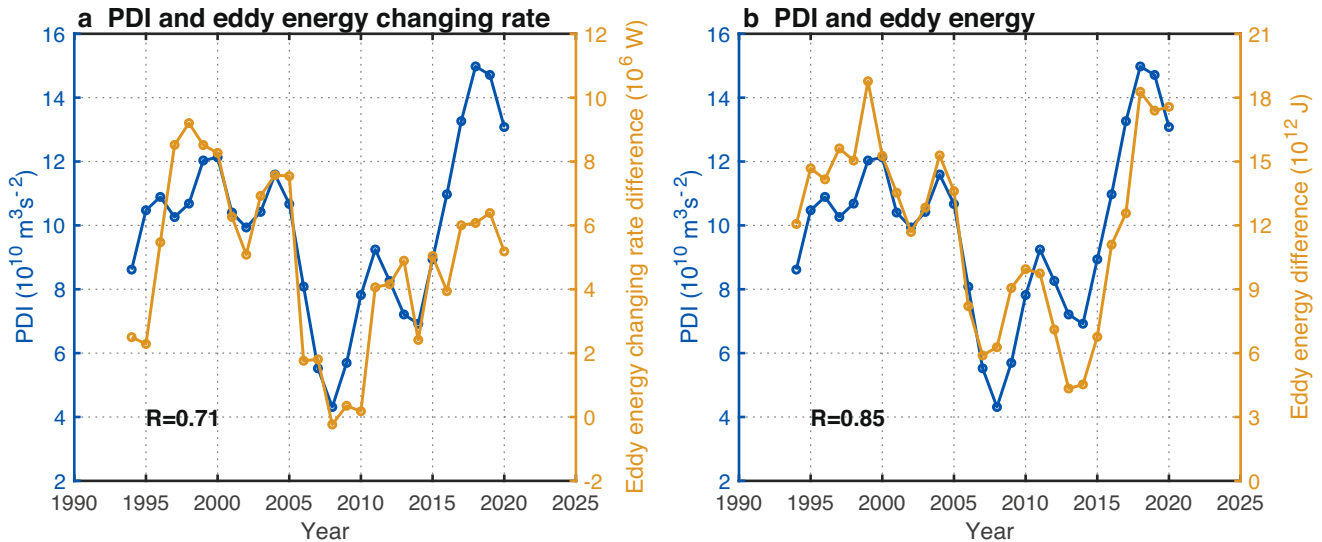


Fig. 3 | Comparison between hurricane intensity and the response of the eddy field within 15 days after hurricanes' passage. a Mean energy changing rate difference between cyclonic and anticyclonic eddies (10^6 W, orange) within 15 days after hurricanes' passage in the Gulf Stream region (GSR), and power dissipation index (PDI) of hurricane in the GSR (10^{10} m³ s⁻², blue) from 1993 to 2021. **b** Same as

a but for the mean energy difference (10^{12} J, orange) between cyclonic and anticyclonic eddies. A 3-year running mean smoothing was applied to all the time series. The correlation coefficients *R* (lower-left corner) are shown in each panel. Source data are provided as a Source Data file.

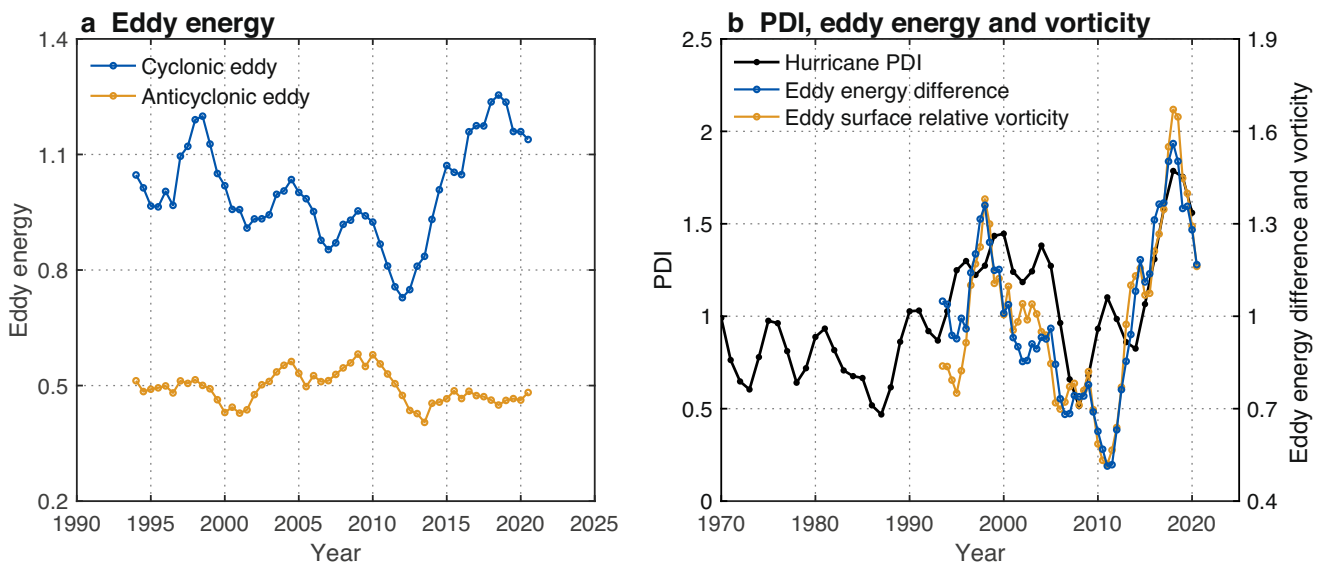


Fig. 4 | Variation of annual mean eddy energy of large eddies and power dissipation index (PDI) in the Gulf Stream region (GSR). a Cyclonic eddy energy (blue) and anticyclonic eddy energy (orange), **b** PDI (black), the energy difference between cyclonic and anticyclonic eddies (blue), and the total surface relative

vorticity of the eddy field (orange) in the GSR from 1993 to 2021. All quantities are normalized by their own mean values. A 3-year running mean smoothing was applied to all the time series. Source data are provided as a Source Data file.

exhibited pronounced variations on interannual to multi-decadal time scales, including a notable lull around 2010, followed by a rapid and substantial fourfold increase within a few years (Fig. 1c and Fig. 4b). With regard to eddies, the energy difference between cyclonic and anticyclonic eddies is significantly correlated with PDI variations ($R > 0.7$, $p < 0.05$) within a 95% confidence interval. Similarly, the eddies' total surface relative vorticity exhibits a strong correlation ($R > 0.7$, $p < 0.05$, Fig. 4b). In conjunction with the direct impact of hurricanes as identified from the short-term response of the eddy field, these results provide compelling evidence that hurricanes are one probable cause of long-term variations in the eddy field of the GSR.

It is also important to note that the hurricane is not the sole factor affecting the eddy field. In particular, around 2010, when hurricane activity is at its lowest level, the energy difference of the eddy field varies out of phase with the hurricane PDI (Fig. 4b), indicating the presence of alternative forces. Among the potential factors, the local wind stress curl and the local buoyancy flux within the GSR can be excluded as possible causes, as both of their variation patterns show minimal resemblance to that of the eddy field (Fig. 5a, b). With respect to the large-scale oceanic features, the GS transport, monitored at 26.5°N by the RAPID project, exhibits a high degree of similarity to the eddies (Fig. 5c), with a correlation exceeding 0.7 at a lead of approximately one

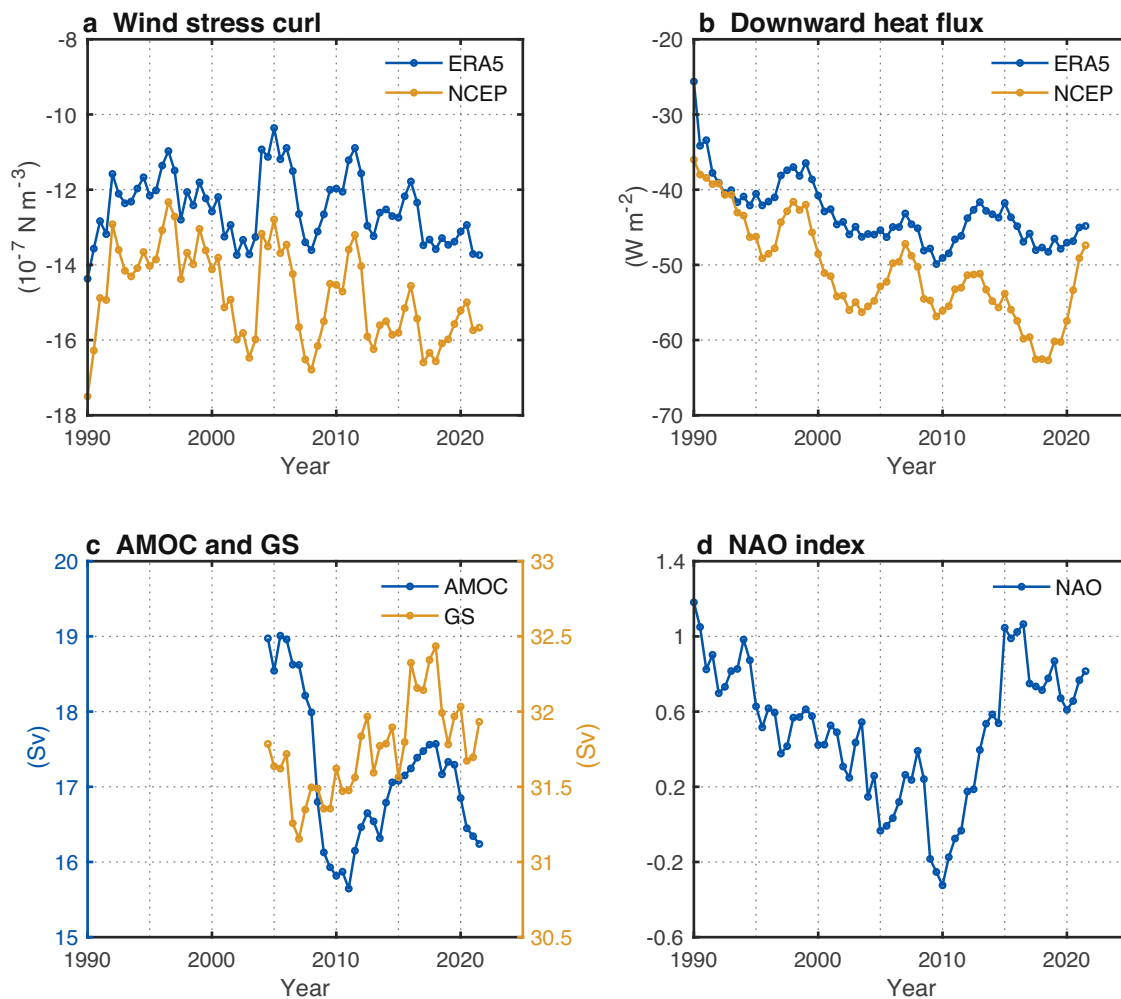


Fig. 5 | Variations of other environmental variables. **a** Wind stress curl (10^{-7} N m^{-3}) in the Gulf Stream region (GSR). **b** Downward surface heatflux (W m^{-2}) in the GSR. **c** The Atlantic meridional overturning circulation (AMOC) strength and the Gulf Stream (GS) transport (Sverdrup, abbreviated as Sv) at 26.5°N for the period

2004–2021. **d** The winter-time North Atlantic Oscillation (NAO) index (from January to March). A 3-year running mean smoothing was applied to all the time series. Source data are provided as a Source Data file.

year. The strength of the AMOC, as observed at 26.5°N , shows a notable decline prior to 2010 and subsequent recovery⁴⁶ (Fig. 5c). However, its correlation with the eddy field is relatively weak, likely due to the abrupt nature of the change. Moreover, there is evidence indicating a connection between the winter-time NAO index and the eddies of GS^{47,48}. Indeed, the time series of the winter-time NAO index exhibits a strong resemblance to that of the eddy field (Fig. 5d), with a correlation exceeding 0.7 at an approximately 2-year lead. These factors- the GS, the AMOC, and the large-scale climate oscillation pattern denoted by the winter-time NAO index-may all have contributed to the observed variation of the energy difference between cyclonic and anticyclonic eddies. However, their respective forcing mechanisms remain uncertain.

Discussion

Isolated mesoscale eddies are capable of transporting mass and climatically important tracers over considerable distances^{7,8}. They are, therefore, considered to play a pivotal role in the global climate system. The processes regulating the properties of the eddy field are of great importance in this regard; however, identifying these processes is a formidable task, particularly given the multitude of potential factors that could influence the eddy field^{47,48}.

Furthermore, the relationships between eddies and some forcing factors are likely mutual, thereby further complicating the task of identifying causality. For example, it's evident that the GS has a strong influence on the eddy field. Meanwhile, beneath the upper layer of GS, the deep western boundary current (DWBC) passes through and crosses with the GS near Cape Hatteras. Previous research has indicated that the eddy fluxes of potential vorticity can entrain the upper DWBC under the GS, consequently altering the path of the GS^{49,50}. This, in turn, can influence the characteristics of the GS.

In view of the above, the forcing mechanism identified in the present study represents a notable advancement in our understanding of the subject matter. The short-term response analysis demonstrated that the hurricane-vorticity and hurricane-mixing mechanism can effectively strengthen cyclonic eddies while simultaneously weakening anticyclonic ones. This distinctive impact, namely, the opposite response of the two kinds of eddies, provides an essential tool for evaluating the role of not only hurricanes but other possible factors in the long-term behavior of the eddy field of the GSR. Furthermore, the knowledge of the inclination of hurricanes to inject positive vorticity into the ocean provides insight into their potential impacts on large-scale ocean circulations and climate, which merits further investigation in the future.

Methods

Theory of vorticity injection by hurricanes

In general, mesoscale eddies are primarily in geostrophic balance and satisfy the geostrophic relation⁵¹,

$$-fv = -\frac{1}{\rho} \frac{\partial p}{\partial x} \quad (1)$$

$$fu = -\frac{1}{\rho} \frac{\partial p}{\partial y} \quad (2)$$

Where f denotes the Coriolis parameter, ρ denotes the sea water density, and p denotes the pressure. Subtracting the y derivative of the Eq. (2) from the x derivative of the Eq. (1) with ignorance of the β effect leads to the equation of relative vorticity (ζ):

$$f\zeta = \frac{1}{\rho} \nabla^2 p \quad (3)$$

Considering the hurricane scenario and defining the eddy field as the deviation from the time-mean field, the vorticity and pressure field can be decomposed into time-mean and eddy components. Thus, we have $\zeta = \bar{\zeta} + \zeta'$, $p = \bar{p} + p'$, where the overbar indicates the time-mean terms and the prime indicates the deviation.

After hurricanes have passed, the atmospheric pressure returns to a normal equilibrium state, and we subtract the large-scale term:

$$f\zeta' = \frac{1}{\rho} \nabla^2 p' = \frac{1}{\rho} \nabla^2 (\rho g \eta') \quad (4)$$

where ζ' denotes the eddy relative vorticity, p' denotes the hurricane atmospheric disturbance and $p' = \rho g \eta'$, η' denotes the sea surface elevation caused by hurricanes. In a stratified ocean, the geostrophic response of η' is predominantly controlled by the isotherm displacement (h')¹⁹ due to the storm-induced upwelling⁵²:

$$\eta' \sim h' \sim \int W_E dt = \int \frac{1}{\rho f} (\nabla \times \boldsymbol{\tau}_H) dt \quad (5)$$

$$f\zeta' \sim \frac{g}{\rho f} \nabla^2 \left(\int (\nabla \times \boldsymbol{\tau}_H) dt \right) \quad (6)$$

Where W_E is the Ekman pumping induced by the hurricane, $\boldsymbol{\tau}_H = (\tau_x, \tau_y)$ is the hurricanes' horizontal wind stress A . This suggests that hurricanes inject vorticity into the ocean through Ekman pumping, causing changes in eddies' relative vorticity. More specifically, in the core of the hurricane, the positive wind stress curl forces upwelling and thus elevates the isopycnal in the ocean. Such lifting is in the same sense as the upward displacements of isopycnals in cyclonic eddies, but is opposite to the isopycnal displacements in anticyclonic eddies. Consequently, if there are preexisting mesoscale eddies in the ocean, the hurricane will enhance the cyclonic eddies but weaken the anticyclonic eddies.

Hurricane intensity

Hurricane dataset for the North Atlantic Ocean is obtained from the International Best Track Archive for Climate Stewardship (IBTrACS, v4r00)^{35,36}, which provides hurricane center position and the 1-min maximum sustained wind speed (V_{max}) at 6-hour intervals.

We use the power dissipation index (PDI) proposed by Emanuel¹⁷ to evaluate the hurricane intensity. For each individual hurricane, PDI

is calculated as follows:

$$PDI = \int_0^\tau V_{max}^3 dt \quad (7)$$

Where τ denotes the hurricane duration. The annual accumulated PDI is the sum of all storms that occurred in a year in a specific region.

Surface eddy energy and eddy relative vorticity

The mesoscale eddy dataset used in this study is the META3.2. Most of the eddy energy is stored in the form of eddy available potential energy, which is defined as the difference in gravitational potential energy between a reference state and the physical state associated with an eddy⁵³. For simplicity, we calculate the eddies' surface available potential energy (SAPE)⁵⁴ to represent the eddy energy:

$$SAPE = \iint \frac{1}{2} \rho g \eta_{eddy}^2 dA \quad (8)$$

Where η_{eddy} denotes the eddy amplitude, calculated as the height difference between the extremum of sea surface height (SSH) within the eddy and the SSH around the eddy edge³⁷, and A denotes the eddy area.

According to Stokes relation⁵¹, the relative vorticity enclosed by the eddy area is equal to the velocity circulation integrated along the eddy perimeter:

$$\zeta_{eddy} = \oint_A \zeta dA = \oint_L \mathbf{u} \cdot d\mathbf{l} = \bar{U} \cdot L \quad (9)$$

Where ζ_{eddy} denotes the eddy's surface relative vorticity, $\mathbf{u} = (u, v)$ is the horizontal rotational velocity of eddy, \bar{U} is the circum-averaged speed of eddy, and L is the eddy perimeter.

Multi-year eddy energy analysis in the hurricane center coordinate

To be consistent with the availability of the META3.2 dataset, only the best-track data starting from 1993 are used in this study. The stage of a hurricane's life cycle in this study is divided into the following three intensity groups, defined on the basis of the Saffir-Simpson Hurricane Scale: TD-TS ($V_{max} < 33ms^{-1}$), Cat 1-2 hurricane ($33ms^{-1} \leq V_{max} < 50ms^{-1}$) and Cat 3-5 hurricane ($V_{max} \geq 50ms^{-1}$). Between 1993-2021 which was covered in the analysis of Fig. 1, there were 231 TD-TS, 98 Cat 1-2 hurricanes and 73 Cat 3-5 hurricanes. During this period, we analyzed all the eddies' lifetime evolution immediately after their meeting with hurricanes in the North Atlantic Ocean in the hurricane center coordinate.

Specifically, for each 6-h storm location in the best-track data, the eddies that were present on the day of the hurricane's arrival are identified. For these selected eddies, we calculate the distance of each eddy from the storm center, and the 15-day averaged eddy energy changing rate after hurricane passage. Ultimately, based on the groups of storm intensity and the distance from the hurricane center, an average over the 1000 km in the radial direction is then performed, retaining the eddy energy changing rate as a function of the radial distance and hurricane intensity.

Year-by-year eddy response

As shown in Fig. 2, the vorticity-injection mechanism is dominant in situations of strong hurricanes. We only considered hurricanes' with $V_{max} \geq 25ms^{-1}$ before their landing. Following the same procedure as in the multi-year analysis, we calculated the mean eddy energy changing rate and energy averaged over a 15-day period following the hurricane-eddy encounter within 3000 km of the hurricane center for each year.

Annual mean eddy field of large eddies

Statistical analysis of eddies in the GSR shows that the lifespan of most large eddies with radii greater than 90 km is in the range of 50–250 days, with an overall mean lifespan of 120 days. The mean lifetimes of cyclonic and anticyclonic large eddies are roughly 130 and 110 days, respectively (Supplementary Fig. 5a). Eddies with radii less than 90 km have much shorter lifetimes, averaging about 30 days for both cyclonic and anticyclonic eddies (Supplementary Fig. 5b). Although these large eddies make up only 20–30% of the total quantity, they account for 70% or more of the total energy of the eddy field in the GSR (Supplementary Fig. 5c, d). We can, therefore, argue that large eddies dominate the eddy energy field and have the ability to maintain the effects of hurricanes in the ocean for a long time. Afterward, we calculated the annual mean energy and surface relative vorticity of those large eddies and compared them with the regional hurricane PDI (Fig. 4).

Correlation analysis

The student's t -test is employed to assess the statistical significance of the results. For correlation tests between two variables, particularly time series after low-pass filtering (e.g., a 3-year running mean smoothing), the degrees of freedom are adjusted to reflect the number of effective degrees of freedom. The following theoretical approximation of the number of effective degrees of freedom (N_{eff}) is used^{55,56}.

$$\frac{1}{N_{eff}} \approx \frac{1}{N} + \frac{2}{N} \sum_{j=1}^L \frac{(N-j)}{N} \rho_{XX}(j) \rho_{YY}(j) \quad (10)$$

Where N is the sample size, $\rho_{XX}(j)$ and $\rho_{YY}(j)$ are the autocorrelations of two sampled time series X and Y at time lag j , respectively and L is the lag step at which the autocorrelations decay to insignificance.

$$r_{crit} = \sqrt{t_{\alpha, N_{eff}}^2 / (t_{\alpha, N_{eff}}^2 + N_{eff})} \quad (11)$$

For a given N_{eff} , the critical value r_{crit} for evaluating the null hypothesis (i.e., the correlation between series X and Y is zero) can be obtained using the t distribution at the chosen significant level α . When the calculated correlation exceeds r_{crit} , the null hypothesis is rejected, signifying that the correlation between series X and Y is statistically significant at the corresponding α level.

Data availability

The hurricane best-track data used in this study is the IBTrACS (v4r00) data, retrieved from the NOAA National Centers for Environmental Information (<https://www.ncei.noaa.gov/products/international-best-track-archive>). The META 3.2 dataset provided by AVISO can be downloaded from <https://www.aviso.altimetry.fr/en/data/products/value-added-products/global-mesoscale-eddy-trajectory-product/meta3-2-dt.html>. Two wind field and surface heat fluxes datasets were used, one is NCEP/NCAR Reanalysis 1 data with the monthly temporal resolution and a $1.875^\circ \times 1.875^\circ$ horizontal resolution (<https://psl.noaa.gov/data/gridded/data.ncep.reanalysis.html>), and the other is the ERA5 with the monthly temporal resolution and a $0.25^\circ \times 0.25^\circ$ horizontal resolution (<https://cds.climate.copernicus.eu/cdsapp#!/dataset/reanalysis-era5-land-monthly-means?tab=overview>). The RAPID-MOCHA-WBTS data was downloaded from <https://rapid.ac.uk/data/data-download>. The monthly NAO index was downloaded from <http://www.cpc.ncep.noaa.gov/products/precip/CWlink/pna/norm.nao.monthly.b5001.current.ascii.table>. The altimeter SLA data provided by CMEMS can be downloaded from https://data.marine.copernicus.eu/product/SEALEVEL_GLO_PHY_L4_MY_008_047/description. Source data are provided with this paper.

Code availability

The code used to analyze these data and generate the results presented in the study can be obtained from <https://doi.org/10.5281/zenodo.14223542>. Matlab 2019 was used to plot the figures.

References

- Sanders, F. Explosive cyclogenesis in the west-central North Atlantic Ocean, 1981-84. Part I: composite structure and mean behavior. *Mon. Weather Rev.* **114**, 1781–1794 (1986).
- Minobe, S., Kuwano-Yoshida, A., Komori, N., Xie, S. P. & Small, R. J. Influence of the Gulf Stream on the troposphere. *Nature* **452**, 206–209 (2008).
- Gaube, P. & McGillicuddy, D. J. The influence of Gulf Stream eddies and meanders on near-surface chlorophyll. *Deep Sea Res.* **122**, 1–16 (2017).
- Zhang, S., Curchitser, E. N., Kang, D., Stock, C. A. & Dussin, R. Impacts of mesoscale eddies on the vertical nitrate flux in the Gulf Stream region. *J. Geophys. Res. Oceans* **123**, 497–513 (2018).
- Hogg, N. G. & Johns, W. E. Western boundary currents. *Rev. Geophys.* **33**, 1311–1334 (2012).
- Buckley, M. W. & Marshall, J. Observations, inferences, and mechanisms of the Atlantic meridional overturning circulation: a review. *Rev. Geophys.* **54**, 5–63 (2016).
- Early, J. J., Samelson, R. M. & Chelton, D. B. The evolution and propagation of quasigeostrophic ocean eddies. *J. Phys. Oceanogr.* **41**, 1535–1555 (2011).
- Zhang, Z., Wang, W. & Qiu, B. Oceanic mass transport by mesoscale eddies. *Science* **345**, 322–324 (2014).
- Hummon, J. M. & Rossby, T. Spatial and temporal evolution of a Gulf Stream crest-warm core ring interaction. *J. Geophys. Res. Oceans* **103**, 2795–2809 (1998).
- Auer, S. J. Five-year climatological survey of the Gulf Stream system and its associated rings. *J. Geophys. Res. Oceans* **92**, 11709–11726 (2012).
- Small, R. J. et al. Air–sea interaction over ocean fronts and eddies. *Dyn. Atmos. Oceans* **45**, 274–319 (2008).
- Ma, X. et al. Western boundary currents regulated by interaction between ocean eddies and the atmosphere. *Nature* **535**, 533–537 (2016).
- Grist, J. P. et al. Future evolution of an eddy rich ocean associated with enhanced east Atlantic storminess in a coupled model projection. *Geophys. Res. Lett.* <https://doi.org/10.1029/2021GL092719> (2021).
- Zhang, Y., Zhang, Z. G., Chen, D., Qiu, B. & Wang, W. Strengthening of the Kuroshio current by intensifying tropical cyclones. *Science* **368**, 988–993 (2020).
- Hart, R. E. & Evans, J. L. A climatology of the extratropical transition of Atlantic tropical cyclones. *J. Clim.* **14**, 546–564 (2001).
- Kossin, J. P., Emanuel, K. A. & Vecchi, G. A. The poleward migration of the location of tropical cyclone maximum intensity. *Nature* **509**, 349–352 (2014).
- Emanuel, K. Increasing destructiveness of tropical cyclones over the past 30 years. *Nature* **436**, 686–688 (2005).
- Ma, Z., Fei, J., Liu, L., Huang, X. & Li, Y. An investigation of the influences of mesoscale ocean eddies on tropical cyclone intensities. *Mon. Weather Rev.* **145**, 1181–1201 (2017).
- Shay, L. K., Goni, G. J. & Black, P. G. Effects of a warm oceanic feature on Hurricane Opal. *Mon. Weather Rev.* **128**, 1366–1383 (2000).
- Lin, I. I. et al. The interaction of Supertyphoon Maemi with a warm ocean eddy. *Mon. Weather Rev.* **133**, 2635–2649 (2005).
- Fujiwara, K. & Kawamura, R. Intensification of a distant hurricane by warm-core eddies in the Gulf Stream in boreal fall. *Atmos. Sci. Lett.* <https://doi.org/10.1002/asl.1141> (2022).
- Shay, L. K. & Jaimes, B. Near-inertial wave wake of hurricanes Katrina and Rita over mesoscale oceanic eddies. *J. Phys. Oceanogr.* **40**, 1320–1337 (2010).
- Sun, L. et al. Effects of super typhoons on cyclonic ocean eddies in the western North Pacific: a satellite data-based evaluation

- between 2000 and 2008. *J. Geophys. Res. Oceans* **119**, 5585–5598 (2014).
24. Shang, X. D., Zhu, H. B., Chen, G. Y., Xu, C. & Yang, Q. Research on cold core eddy change and phytoplankton bloom induced by typhoons: case studies in the South China Sea. *Adv. Meteorol.* **2015**, 1–19 (2015).
25. D'Asaro, E. A., Sanford, T. B., Niiler, P. P., & Terrill, E. J. Cold wake of hurricane Frances. *Geophys. Res. Lett.* **34**, L15609 (2007).
26. Vincent, E. M. et al. Processes setting the characteristics of sea surface cooling induced by tropical cyclones. *J. Geophys. Res. Oceans* **117**, C02020 (2012).
27. Ezer, T., Atkinson, L. P. & Tuleya, R. Observations and operational model simulations reveal the impact of hurricane Matthew (2016) on the Gulf Stream and coastal sea level. *Dyn. Atmos. Oceans* **80**, 124–138 (2017).
28. Ezer, T. Numerical modeling of the impact of hurricanes on ocean dynamics: sensitivity of the Gulf Stream response to storm's track. *Ocean Dyn.* **69**, 1053–1066 (2019).
29. Ezer, T. The long-term and far-reaching impact of hurricane Dorian (2019) on the Gulf Stream and the coast. *J. Mar. Syst.* **208**, 103370 (2020).
30. Todd, R. E., Asher, T. G., Heiderich, J., Bane, J. M. & Luettich, R. A. Transient response of the Gulf Stream to multiple hurricanes in 2017. *Geophys. Res. Lett.* **45**, 10,509–10,519 (2018).
31. Cronin, M. & Watts, D. R. Eddy-mean flow interaction in the Gulf Stream at 68° W. Part I: eddy energetics. *J. Phys. Oceanogr.* **26**, 2107–2131 (1996).
32. Kang, D. & Curchitser, E. N. Energetics of eddy-mean flow interactions in the Gulf Stream region. *J. Phys. Oceanogr.* **45**, 1103–1120 (2015).
33. Elsner, J. B., Kossin, J. P. & Jagger, T. H. The increasing intensity of the strongest tropical cyclones. *Nature* **455**, 92–95 (2008).
34. Emanuel, K. Atlantic tropical cyclones downscaled from climate reanalyses show increasing activity over past 150 years. *Nat. Commun.* **12**, 7027 (2021).
35. Knapp, K. R., Kruk, M. C., Levinson, D. H., Diamond, H. J. & Neumann, C. J. The international best track archive for climate stewardship (IBTrACS): unifying tropical cyclone best track data. *Bull. Am. Meteor. Soc.* **91**, 363–376 (2010).
36. Gahtan, J. et al. International best track archive for climate stewardship (IBTrACS) project, version 4r01. NOAA National Centers for Environmental Information. <https://www.ncei.noaa.gov/access/metadata/landing-page/bin/iso?id=gov.noaa.ncdc:C01552> (2024).
37. Pegliasco, C. et al. META3.1exp: a new global mesoscale eddy trajectory atlas derived from altimetry. *Earth Syst. Sci. Data* **14**, 1087–1107 (2022).
38. Hersbach, H. et al. The ERA5 global reanalysis. *Q. J. R. Meteorol. Soc.* **146**, 1999–2049 (2020).
39. Kalnay et al. The NCEP/NCAR 40-year reanalysis project. *Bull. Am. Meteor. Soc.* **77**, 437–470 (1996).
40. Moat B. I. et al. Atlantic meridional overturning circulation observed by the RAPID-MOCHA-WBTS (RAPID-Meridional Overturning Circulation and Heatflux Array-Western Boundary Time Series) array at 26N from 2004 to 2023 (v2023.1). British Oceanographic Data Centre - Natural Environment Research Council (2024).
41. Barnston, A. G. & Livezey, R. E. Classification, seasonality and persistence of low-frequency atmospheric circulation patterns. *Mon. Weather Rev.* **115**, 1083–1126 (1987).
42. Lu, Z., Wang, G. & Shang, X. Response of a preexisting cyclonic ocean eddy to a typhoon. *J. Phys. Oceanogr.* **46**, 2403–2410 (2016).
43. Huang, X. & Wang, G. Response of a mesoscale dipole eddy to the passage of a tropical cyclone: a case study using satellite observations and numerical modeling. *Remote Sens.* **14**, 2865 (2022).
44. Lu, Z., Wang, G., Shang, X. & Xie, X. Uncertainties in altimetry observations of eddy changes induced by tropical cyclones. *J. Phys. Oceanogr.* **53**, 113–129 (2023).
45. Chelton, D. B., Schlax, M. G. & Samelson, R. M. Global observations of nonlinear mesoscale eddies. *Prog. Oceanogr.* **91**, 167–216 (2011).
46. Smeed, D. A. et al. Observed decline of the Atlantic meridional overturning circulation 2004–2012. *Ocean Sci.* **10**, 29–38 (2014).
47. Chaudhuri, A. H., Gangopadhyay, A. & Bisagni, J. J. Interannual variability of Gulf Stream warm-core rings in response to the North Atlantic oscillation. *Cont. Shelf Res.* **29**, 856–869 (2009).
48. Penduff, T., Barnier, B., Dewar, W. K. & O'Brien, J. J. Dynamical response of the oceanic eddy field to the North Atlantic oscillation: a model–data comparison. *J. Phys. Oceanogr.* **34**, 2615–2629 (2004).
49. Spall, M. A. Dynamics of the Gulf Stream/deep western boundary current crossover. Part I: entrainment and recirculation. *J. Phys. Oceanogr.* **26**, 2152–2168 (1996).
50. Thompson, J. D. & Schmitz, W. J. Jr A limited-area model of the Gulf Stream: design, initial experiments, and model-data inter-comparison. *J. Phys. Oceanogr.* **19**, 791–814 (1989).
51. Pedlosky, J. *Ocean Circulation Theory* (Springer Science & Business Media, 1996).
52. Gill, A. E. *Atmosphere-Ocean Dynamics* (Academic, 1982).
53. Xu, C., Shang, X. D. & Huang, R. X. Estimate of eddy energy generation/dissipation rate in the world ocean from altimetry data. *Ocean Dyn.* **61**, 525–541 (2011).
54. Huang, R., Qiu, B. & Jing, Z. Surface available gravitational potential energy in the world oceans. *Acta Oceanol. Sin.* **41**, 40–56 (2022).
55. Pyper, B. J. & Peterman, R. M. Comparison of methods to account for autocorrelation in correlation analyses of fish data. *Can. J. Fish. Aquat. Sci.* **55**, 2127–2140 (1998).
56. Li, Y., Li, J. & Feng, J. A teleconnection between the reduction of rainfall in southwest Western Australia and north China. *J. Clim.* **25**, 8444–8461 (2012).

Acknowledgements

This work was supported by the National Natural Science Foundation of China through Grant 42288101 of Y. Zhang and W. Wang.

Author contributions

Y.Z. and W.W. conceived the project and developed a data analysis methodology. X.N. carried out data analyses and wrote the manuscript. Y.Z. and W.W. reviewed and edited the manuscript.

Competing interests

The authors declare no competing interests.

Additional information

Supplementary information The online version contains supplementary material available at <https://doi.org/10.1038/s41467-025-55927-6>.

Correspondence and requests for materials should be addressed to Yu Zhang or Wei Wang.

Peer review information *Nature Communications* thanks Tal Ezer and the other, anonymous, reviewer for their contribution to the peer review of this work. A peer review file is available.

Reprints and permissions information is available at <http://www.nature.com/reprints>

Publisher's note Springer Nature remains neutral with regard to jurisdictional claims in published maps and institutional affiliations.

Open Access This article is licensed under a Creative Commons Attribution-NonCommercial-NoDerivatives 4.0 International License, which permits any non-commercial use, sharing, distribution and reproduction in any medium or format, as long as you give appropriate credit to the original author(s) and the source, provide a link to the Creative Commons licence, and indicate if you modified the licensed material. You do not have permission under this licence to share adapted material derived from this article or parts of it. The images or other third party material in this article are included in the article's Creative Commons licence, unless indicated otherwise in a credit line to the material. If material is not included in the article's Creative Commons licence and your intended use is not permitted by statutory regulation or exceeds the permitted use, you will need to obtain permission directly from the copyright holder. To view a copy of this licence, visit <http://creativecommons.org/licenses/by-nc-nd/4.0/>.

© The Author(s) 2025